Ab initio calculation of melting and thermodynamic properties of crystal and liquid aluminum

Galen K. Straub, John B. Aidun, John M. Wills, Carlos R. Sanchez-Castro, and Duane C. Wallace
Los Alamos National Laboratory, Los Alamos, New Mexico 87545
(Received 1 April 1994)

A first-principles technique for calculating accurate equations of state of metals is illustrated with an application to Al. Results for the thermodynamic properties of Al at densities near normal, and at temperatures into the liquid phase, are presented. In contrast to previous calculations by other workers, the present technique makes no use of experimental data. The *ab initio* procedure begins with electronic-band-structure calculation of the ground-state energy, the elastic constants, and selected short-wavelength phonons. A physically realistic interatomic potential is calibrated by fitting it to the calculated elastic constants and phonons. Ion-motional contributions are computed from quasiharmonic lattice dynamics at low temperatures, and from molecular-dynamics simulations at classical temperatures. Melting is computed from the free energy constructed from these combined results. Very accurate results are obtained for zero-temperature properties and phonon frequencies. The calculated melting temperature of 955 K is within 2.5% of the observed value, a difference comparable to the estimated precision of the calculation. Good results are obtained for two highly sensitive quantities, the entropy change upon melting and the Clapeyron slope. The calculated entropy as a function of temperature is in excellent agreement with experiment for solid and liquid phases. The present procedure can potentially provide reliable values of thermodynamic properties of any metal under extreme conditions where no data are avilable.

I. INTRODUCTION

At Los Alamos, we have undertaken research in techniques to calculate accurate equations of state for metals, from first principles, without recourse to any experimental data whatsoever. Our region of interest includes densities from normal to two or three times normal, and temperatures up to several times melting. Under these conditions, the Born-Oppenheimer approximation[1] is a proper starting point, with the electronic ground state serving as a potential for the ion motion, and with thermal excitation of the valence electrons treated as a free-energy perturbation.[2] The following three steps comprise the most reliable procedure available for *ab initio* calculations.

(a) Calculate the ground-state energy, the elastic constants, and a few zone-boundary phonons, as functions of compression using band-structure theory.

(b) Construct a physically realistic interatomic potential, and calibrate it with the calculated elastic constants and zone-boundary phonons.

(c) Evaluate the ion-motional contribution to thermodynamic functions by means of quasiharmonic lattice dynamics at low temperatures, and by means of the molecular-dynamics (MD) technique at temperatures where the ion motion is classical.

Melting is computed from the free energy constructed from the results of these three steps.

The present paper presents our results for Al at densities near normal, and at temperatures well into the liquid regime.

Several previous calculations of melting in aluminum have been reported. Moriarty, Young and Ross[3] used generalized pseudopotential theory, and evaluated the crystal free energy from quasiharmonic lattice dynamics, and the liquid free energy from fluid variational theory, to calculate the melting curve of fcc Al to the vicinity of 2 Mbar. Their results are in good agreement with experiment. Pélissier[4] used local pseudopotential theory fitted to experimental data, and free-energy approximations similar to those of Moriarty, Young, and Ross,[3] to calculate the melting curve of fcc Al to 2 Mbar. The melting curve of Pélissier agrees well with that of Moriarty, Young, and Ross. Mei and Davenport[5] used embedded-atom potentials, with a large number of parameters fitted to experimental data, and with crystal and liquid free energies evaluated by molecular dynamics, to calculate the melting temperature of fcc Al at zero pressure. Our procedure bears some similarities to and some differences from these calculations. The most significant differences are that our interionic potential is fitted to information obtained entirely from band-structure calculations, making no use of experimental data, and our free energies at classical temperatures are evaluated entirely from MD simulations without recourse to approximations.

In the following section, the band-structure calculations are described, and the resulting zero-temperature equation of state and four zone-boundary phonons are compared with experiment. Section III describes the calibration of the volume-dependent, two-body interatomic potential, and compares three calculated moments of the phonon spectrum with experiment. Evaluation of the ion-motional contribution to thermodynamic functions, for crystal and liquid phases, is carried out in Sec. IV. The complete Hamiltonian and complete free energy are given in Sec. V, and theory and experiment are compared for the melting properties, crystal anharmonicity,

and entropy at temperatures to twice melting. Finally, in Sec. VI, it is argued that our procedure shows promise for reliable calculations of thermodynamic properties of metals under extreme conditions.

II. BAND-STRUCTURE CALCULATIONS

The electronic structure calculations were performed with a full-potential, augmented linear muffin-tin orbital band-structure method.[6] This method has previously been successfully used to calculate elastic constants of transition metals.[7] The calculations were all-electron, scalar relativistic, and used the Hedin-Lundqvist exchange-correlation functional.[8] The basis functions were Bloch linear combinations of augmented, linear muffin-tin orbitals through $l=2$. Inside the muffin-tin spheres, basis function were expanded in spherical waves through $l=8$; harmonic expansions of the electron density and potential were carried out through $l=8$. In the interstitial region, Fourier expansions were cut off at $g_{\max}\sim 5.5V^{1/3}/2\pi$ for the electron density and potential, and at $g_{\max}\sim 3.2V^{1/3}/2\pi$ for the basis functions; V is the unit-cell volume. Integrations over the Brillouin zone (BZ) were performed using special points with Gaussian broadening; the width of the Gaussian was 65 mRy.[9]

The energy of the fcc structure was calculated at 19 volumes ranging from $1.43V_0$ to $0.33V_0$, where V_0 is the room-temperature, experimental unit-cell volume. The equilibrium volume, the bulk modulus, and its pressure derivative are compared with experiment in Table I. The BZ mesh contained 60 points in an irreducible wedge, corresponding to 2048 points in the full zone; convergence was checked at several volumes to 16 384 points in the full zone.

Longitudinal and transverse phonons at the L and X points were calculated at five volumes ranging from V_0 to $0.33V_0$. Total energies were calculated as a function of atomic displacement from equilibrium in doubled unit cells. At each volume, these calculations were performed at four displacement magnitudes to obtain each phonon frequency. Maximum energy differences for the different modes fell approximately in the range 0.05–0.32 mRy near equilibrium and 0.33–2.8 mRy at $0.33V_0$. Gridding of reciprocal space identical to the fcc calculations was used. This corresponded to 1024 points in the full BZ. Convergence was checked up to 8192 points in the full zone at one volume near equilibrium.

The ground-state energy $\Phi_0(V)$ was fitted to a Birch-Murnaghan equation of state[10]

$$\Phi_0(V)=c_0+V_b\sum_{n=2}^{5}\frac{c_n}{n!}\psi^n , \tag{1}$$

where

$$\psi=\frac{1}{2}\left[\left[\frac{V}{V_b}\right]^{-2/3}-1\right] . \tag{2}$$

Values of the parameters V_b and c_n are given in the Appendix.

At zero temperature, $T=0$, the crystal energy in quasiharmonic lattice dynamics is

$$U_0(V)=\Phi_0(V)+E_H(V) , \tag{3}$$

where E_H is the quasiharmonic zero-point vibrational energy,

$$E_H=\tfrac{3}{2}\langle\hbar\omega_\kappa\rangle_{\rm BZ}=\tfrac{9}{8}k\theta_1 . \tag{4}$$

ω_κ are the quasiharmonic phonon frequencies, $\langle\ \rangle_{\rm BZ}$ indicates a Brillouin-zone average, and the second equality in (4) defines the characteristic temperature $\theta_1(V)$. Our evaluation of $\theta_1(V)$ is described in Sec. III. The pressure at $T=0$ is $P_0(V)$,

$$P_0(V)=-dU_0/dV , \tag{5}$$

and the bulk modulus is $B_0(V)$,

$$B_0(V)=-V(dP_0/dV) . \tag{6}$$

Results from the band-structure calculations at zero temperature and pressure are compared with experiment in Table I. The zero-point vibrational energy expands the crystal about 1%, raises the energy 1%, and causes the bulk modulus to decrease by around 2.5%. The agreement of theory and experiment is overall quite good.

Energies of quasiharmonic phonons at points X and L in the fcc BZ were calculated at three volumes and the corresponding frequencies are listed in Table II. Neutron-scattering measurements of the phonon frequencies at 80 K, where $V=110.7a_0^3$, are also listed in Table II. While the theoretical frequencies are uniformly lower than experiment by a few percent, the agreement is, nevertheless, impressively good.

To calculate the complete free energy of Al, in crystal or liquid phases, we will need the contribution due to thermal excitation of the valence electrons from their ground state. Since this contribution is small, an approximation will suffice. In Fig. 1, our calculated electronic density of states is compared with the value for free electrons; from this comparison we conclude that the free-

TABLE I. Comparison of theory and experiment at zero temperature and pressure.

Quantity	Neglecting E_H	Including E_H Φ_0	E_H	Total	Experiment
V (a_0^3)	106.3			107.3	110.6
U_0 (mRy)	−288	−288	3	−285	−249[a]
B_0 (GPa)	84.6	81.1	1.3	82.4	79.4[b]
					82.0[c]
dB_0/dP	4.58	4.65	0.01	4.66	4.72[d]
					4.42[e]

[a]C. Kittel, *Introduction to Solid State Physics*, 5th ed. (Wiley, New York, 1976), p. 74.
[b]G. N. Kamm and G. A. Alers, J. Appl. Phys. **35**, 327 (1964).
[c]J. Vallin, M. Mongy, K. Salama, and O. Beckman, J. Appl. Phys. **35**, 1825 (1964).
[d]P. S. Ho and A. L. Ruoff, J. Appl. Phys. **40**, 3151 (1969), at 77.4 K.
[e]J. F. Thomas, Jr., Phys. Rev. **175**, 955 (1968), at room temperature.

TABLE II. Longitudinal (l) and transverse (t) phonon frequencies, in THz, at X and L points for fcc Al. Theoretical values are given for three atomic volumes, and interpolated theoretical values are compared with neutron scattering measurements at $V=110.7a_0^3$.

V (a_0^3)	$X(l)$	$X(t)$	$L(l)$	$L(t)$
111.970	57.9	33.9	57.3	23.9
106.649	63.1	38.2	63.1	26.9
93.318	78.3	50.7	80.2	35.4
110.7(theory)	59.1	34.9	58.6	24.6
110.7(experiment)[a]	60.9	36.4	60.9	26.3

[a]Reference 23 and data of R. Stedman and G. Nilsson, Phys. Rev. **145**, 492 (1966).

TABLE III. Pseudopotential parameters, characteristic temperatures for crystal (θ_n) and liquid (η_0), and the crystal Grüneisen parameter (γ_0), for Al at three atomic volumes.

Quantity	V (a_0^3) 111.970	106.649	93.318
r_c (a_0)	1.129	1.128	1.123
ξ	1.224	1.160	1.004
θ_0 (K)	278.1	304.6	381.4
θ_1 (K)	386.6	423.8	532.0
θ_2 (K)	387.2	424.9	534.5
η_0 (K)	201.0	217.7	268.7
γ_0	1.92	1.82	1.58

electron model gives an acceptable approximation to the electronic free energy at all volumes and temperatures considered in this study.

III. THE INTERATOMIC POTENTIAL

Aluminum at normal density is a nearly-free-electron metal. Pseudopotential perturbation theory, using an Ashcroft pseudopotential with core radius as the only adjustable parameter, gives an excellent description of the phonon dispersion curves at 80 K.[11] The weakest part of this model is that the calculated bulk modulus is around 30% smaller than the experimental value.[12] The removal of this discrepancy might well be found in higher-order perturbation theory, since it is known that, in a given order of pseudopotential perturbation, the methods of long waves and homogeneous deformation yield different results for the bulk modulus.[13,14] However, in the present work, in order to construct a simple but physically realistic interatomic potential for Al, we will retain the second-order pseudopotential theory, but will vary the Hubbard screening parameter ξ so as to obtain approximate agreement between the long-wavelength phonons and the bulk modulus. This procedure has physical justification since ξ appears in an approximate screening correction due to valence electron exchange and correlation effects, and in the long-wavelength limit ξ controls the valence electron compressibility.[13,15]

The pseudopotential formulation of the real space interatomic potential $\phi(r)$ has been given previously.[16] Here we use the Ashcroft empty core model,[17] with core radius r_c and screening parameter ξ. These parameters are adjusted to provide an overall best fit of the phonons and bulk modulus calculated from the resulting interatomic potential to the four zone-boundary phonons (Table II) and bulk modulus determined by the band-structure calculations. The final values of r_c and ξ are listed in Table III. These may be compared with our earlier results[11] for Al at $V=110.6a_0^3$: $\xi=1.90$, the uniform electron gas value; $r_c=1.117a_0$. While r_c is only weakly dependent upon the fitting procedure and the volume of Al, the parameter ξ must be decreased significantly to give a more accurate value of B_0. This behavior of ξ occurs because there is a slight admixture of d electrons near the Fermi surface, an effect which increases as the volume decreases.[18,19] To extend this study of Al to higher compressions, we are currently developing an interatomic potential that explicitly accounts for the d-electron contribution.

The interatomic potentials at three volumes are shown in Fig. 2. These potentials are quite different from our earlier potential,[20] yet the overall agreement with measured phonon dispersion curves is nearly as good.[11] Since $\phi(r)$ will be the basis for calculating thermodynamic properties due to the motion of the ions, an important check on it is to see how well it gives moments of the phonon distribution. The important moments are expressed by the characteristic temperatures θ_n for $n=0$, 1, 2; θ_1 is given by Eq. (4) and relates to zero-point vibrational energy; θ_0 expresses the quasiharmonic phonon entropy at high temperature,[21]

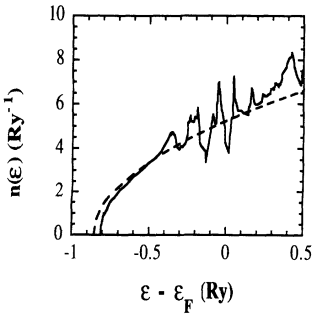

FIG. 1. Calculated electronic density of states for Al (solid) compared with the free electron model (dashed).

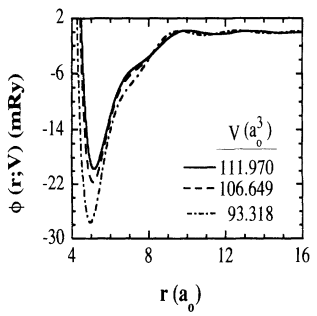

FIG. 2. Pair interaction contribution to the interatomic potentials for Al used in the MD simulations.

$$\ln(k\theta_0)=\langle \ln(\hbar\omega_\kappa)\rangle_{BZ} \; ; \tag{7}$$

and θ_2 expresses leading-order quantum corrections at high temperature,[22]

$$k\theta_2=[\tfrac{5}{3}\langle \hbar^2\omega_\kappa^2\rangle_{BZ}]^{1/2} \; . \tag{8}$$

Experimental phonon moments for Al at 80 K, based on Born–von Karman fits to neutron-scattering data,[23] compare well with our calculated values at the appropriate atomic volume of $110.7a_0^3$:

	Experiment[23]	Theory	% error
θ_0 (K)	283.5	284.2	0.2
θ_1 (K)	399	395	−1.0
θ_2 (K)	404	396	−2.0

Theoretical results for θ_0, θ_1, θ_2, and γ_0 at three volumes are listed in Table III, where the Grüneisen parameter γ_0 is

$$\gamma_0=-\frac{d\ln\theta_0}{d\ln V} \; . \tag{9}$$

IV. MOLECULAR DYNAMICS

We have previously carried out lattice dynamic and constant (N,V,E) MD calculations for metallic sodium in the solid phase,[16,24,25] the liquid phase,[26] and along the solid-liquid boundary,[27] and have provided several studies of statistical mechanical theory useful for interpreting the computer simulations.[28–30] Our conclusion from this work is that the combination of lattice dynamics and molecular dynamics yields accurate results for thermodynamic properties of solids and liquids. Here we carry out this computational program for Al making use of all the techniques developed earlier. The essential difference is that our Al potential is calibrated to band-structure calculations at several volumes, while our Na potential was calibrated to experimental data.[31]

The molecular-dynamics Hamiltonian is H_{MD}

$$H_{MD}=\sum\frac{p^2}{2M}+\sum\phi-\left[\sum\phi\right]_0 , \tag{10}$$

where p is the particle momentum, M is the particle mass, $\phi=\phi(r;V)$ is the volume-dependent interatomic pair potential, the kinetic energy is summed over all particles, the potential is summed over all distinct pairs, and $(\sum\phi)_0$ is the total pair potential evaluated for the perfect crystal configuration. ϕ was tapered to zero with zero slope beyond the ninth fcc shell of neighbors. For every volume, the zero of H_{MD} is the static crystal configuration, which is the classical ground state. The MD calculations were started from the fcc crystal configuration, with a random distribution of velocities, and the system reached equilibrium either in fcc or liquid states. Periodic boundary conditions were applied, and the fixed number of particles used in a simulation ranged from 864 to 4032. Error estimates were obtained from the procedures outlined by Schiferl and Wallace.[32] Results for the MD energy and pressure as functions of volume and temperature are shown in Figs. 3 and 4.

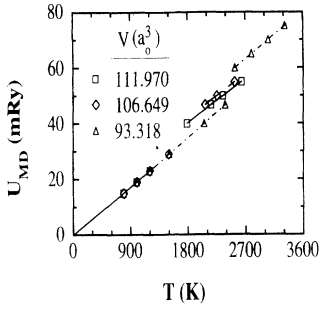

FIG. 3. Thermal contributions to the internal energy determined from MD simulations and thermodynamic fits [Eqs. (13) and (A10)] to them (lines).

To analyze the MD results for the crystalline state, we refer to lattice dynamics theory to write the crystal free energy per atom F^c_{MD}, in the high-temperature (classical) limit as

$$F^c_{MD}=-3kT\ln(T/\theta_0)+F^c_A \; , \tag{11}$$

where $\theta_0(V)$ is listed in Table III, and the variable function F^c_A, which expresses anharmonicity, is taken to be

$$F^c_A=A^c(V)T^3 \; . \tag{12}$$

Then the crystal internal energy per atom U, the entropy per atom S, and the pressure P are given by

$$U^c_{MD}=3kT-2A^cT^3 \; , \tag{13}$$

$$S^c_{MD}=3k[\ln(T/\theta_0)+1]-3A^cT^2 \; , \tag{14}$$

$$VP^c_{MD}=3kT\gamma_0-(dA^c/d\ln V)T^3 \; , \tag{15}$$

where $\gamma_0(V)$ is defined by Eq. (9) and is listed in Table III. Equations (13) and (15) accurately fit our MD results for energy and pressure (see Figs. 3 and 4), with A^c a smooth function of V, small in magnitude. The anharmonic contributions to energy and pressure turn out to be at most 2% of the quasiharmonic contributions. It should be stressed that, since F^c_A is a variable function of V and T, and since it is fitted to the classical MD calculations of energy and pressure, the only error in F^c_{MD} of Eq. (11) is that it omits the quantum contribution to F^c_A, and

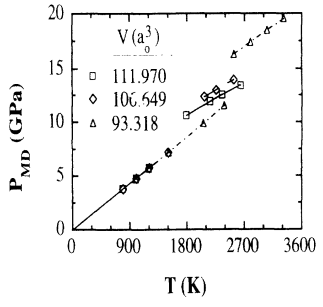

FIG. 4. Thermal contributions to the pressure determined from MD simulations and thermodynamic fits [Eqs. (15) and (A9)] to them (lines).

this contribution is of relative order $(\theta_2/T)^2$, and so is negligible at high temperature.[33]

To analyze the MD results for the liquid state, we write the liquid free energy per atom $F^l_{\rm MD}$ in the form

$$F^l_{\rm MD}=\chi_0(V)-3kT\ln[T/\eta_0(V)]+A^l(V)T^3 . \quad (16)$$

The corresponding internal energy and pressure are again accurately fitted to the MD data, yielding smooth curves of the volume-dependent functions χ_0, η_0, and A^l, where one undetermined entropy constant remains in the η_0 curve. Again, the "anharmonic" terms, coming from A^lT^3 in the free energy, turn out to be at most a few percent of the "quasiharmonic" terms, coming from $ln(T/\eta_0)$ in the free energy. The liquid entropy per atom is

$$S^l_{\rm MD}=3k[\ln(T/\eta_0)+1]-3A^lT^2 . \quad (17)$$

The entropy constant for the liquid state was determined from a constant-volume integration from the virial regime, using previously described techniques.[27,28] The method consists in calculating the entropy at a very high temperature, $T_{\rm max}$, from the virial expansion, and then extending this result to lower temperatures by using the thermodynamic identity

$$S(T)-S(T_{\rm max})=\frac{U_{\rm MD}(T)}{T}-\frac{U_{\rm MD}(T_{\rm max})}{T_{\rm max}}+\int_{T_{\rm max}}^{T}dT'\frac{U_{\rm MD}(T')}{T'^2} \quad (18)$$

at fixed V and N. $U_{\rm MD}$ is determined from molecular-dynamics simulations. Further details of this calculation will be published separately.[34] The resulting values of $\eta_0(V)$ are listed in Table III. The final forms of the functions in Eqs. (11)–(17), which were determined by fitting the MD energy and pressure, are given in the Appendix.

V. COMPLETE THERMODYNAMIC FUNCTIONS

The complete Hamiltonian H is the sum of terms discussed in the preceding sections, namely, the static lattice energy Φ_0 from band-structure calculations, the ion-motional energy $H_{\rm MD}$, and the energy H_E of excitation of valence electrons from their ground state:

$$H=\Phi_0+H_{\rm MD}+H_E . \quad (19)$$

The corresponding Helmholtz free energy F is

$$F=\Phi_0+F_{\rm MD}+F_E . \quad (20)$$

For Al near normal densities, F_E gives a very small contribution and, as demonstrated by Fig. 1, it is adequately approximated by the low-temperature limit of free electron theory:

$$F_E=-\tfrac{1}{6}\pi^2k^2n(\varepsilon_F) , \quad (21)$$

where $n(\varepsilon_F)$ is the density of electronic states at the Fermi energy. From the total free energy, thermodynamic functions were calculated in the region of the volumes listed in Tables II and III; note that the largest volume of $111.970a_0^3$ corresponds to Al at room temperature and zero pressure.

The melting temperature was calculated by equating Gibbs free energies and pressures of crystal and liquid, at a common temperature, and the results at zero pressure are listed in Table IV. Our calculated melting temperature of $T_m=955$ K agrees well with the measured value of 933.45 K. Numerical errors in T_m, from all sources excepting possible errors in our potentials Φ_0 and $\phi(r)$, are estimated at less than $\pm2\%$, or ±19 K. Calculated values of ΔS_m and dT_m/dP are lower than experiment by 19% and by 25–30%, respectively. We attribute these discrepancies to small inaccuracies in Φ_0 and $\phi(r)$, as discussed in the following section.

It should be noted that in the present formulation of the total Hamiltonian, where $\Phi_0(V)$ is separated from $H_{\rm MD}$, the actual melting temperature is different from the temperature at which the constant-volume molecular-dynamics system melts. This is because actual melting at constant pressure is accompanied by a volume change and the corresponding change in $\Phi_0(V)$ is important in the free-energy balance between crystal and liquid. The theoretical contributions to ΔU, the change in internal energy upon melting, are listed in Table IV, and it is seen that $\Delta\Phi_0$ is an important part of the total ΔU.

It has long been known that explicit anharmonicity in crystalline aluminum is extremely small.[35–37] An extensive analysis of currently available experimental data yields the following ratios of anharmonic to quasiharmonic contributions, for temperatures to melting: $\approx0.2\%$ for the entropy; $\approx0.5\%$ for the thermal energy; $\lesssim2\%$ for the pressure. Within errors of the analysis, these values are zero. At comparable densities, our MD calculations give $\lesssim1\%$ for all these ratios. Hence, in agreement with experiment, our theory predicts extremely small anharmonicity in fcc Al at densities near normal and temperatures to melting.

Our classical calculation of the entropy is compared in Fig. 5 with experimental data for crystal and liquid from 300 to 1800 K. The theoretical results are evaluated at the experimental zero-pressure volume, and are lower than experiment by about 1% in the crystal and 2% in

TABLE IV. Comparison of theoretical and experimental melting properties of aluminum.

Quantity	Theory	Experiment
T_m (K)	955	933.45
$\Delta S_m/k$	1.12	1.38[a]
dT_m/dP (K/GPa)	45	61[b]
	45	65[c]
$\Delta\Phi_0$ (mRy)	1.82	
$\Delta U_{\rm MD}$ (mRy)	5.01	
ΔU_E (mRy)	0.01	
ΔU (mRy)	6.84	8.16[a]

[a]M. W. Chase, Jr., C. A. Davies, J. R. Downey, Jr., D. J. Frurip, R. A. McDonald, and A. N. Syverud, J. Phys. Chem. Ref. Data Suppl. **14**, 1 (1985).
[b]Calculated from the Clapeyron equation with $\Delta V/V=0.066$.
[c]J. F. Cannon, J. Phys. Chem. Ref. Data **3**, 781 (1974).

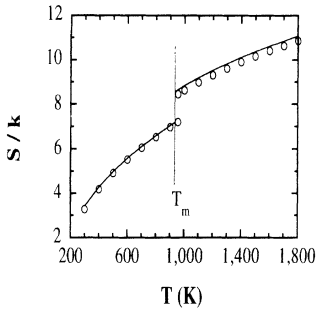

FIG. 5. Measured Al entropy values (lines) compared with classical calculation (dots).

the liquid. If instead we evaluate the entropy at the *calculated* zero-pressure volume, the theoretical results are lower than experiment by 5% in the crystal and 7% in the liquid. As temperature decreases below 400 K, the theoretical entropy begins to depart from the experimental curve because of quantum effects. We omit consideration of the quantum regime here, since it is well established that quasiharmonic lattice dynamics gives excellent results in the quantum regime.[2,16,36]

VI. DISCUSSION

In order to evaluate our theoretical procedure, let us first discuss the application presented here to metallic aluminum. Our input data consist of band-structure calculations of the static lattice potential Φ_0 and of the energies of several short-wavelength phonons. A two-body potential ϕ is introduced and is calibrated to the short-wavelength phonons, and to a combination of long-wavelength phonons, namely, the bulk modulus. Hence ϕ should give an accurate description of all small distortions from the fcc lattice for real aluminum; that it does so is evidenced by the accurate Al phonon spectrum obtained from ϕ. Furthermore, in principle, ϕ should *approximately* account for *large* distortions from the fcc lattice, including the far-from-crystalline structures found in the liquid phase. This principle is clearly satisfied, as evidenced by the agreement between theory and experiment for Al at temperatures to twice melting (see Fig. 5). Nevertheless, the potential ϕ might very well be less accurate for larger distortions from the fcc lattice than for smaller ones. We believe that this is the case, and that this small error, together with a small error in Φ_0, is responsible for the errors of around 20–30 % in our calculated values of the very sensitive melting quantities ΔS_m and dT_m/dP (Table IV).

Considering our procedure in general, as it might be applied to any metal, both the band-structure calculations and the molecular-dynamic calculations are expected to be accurate. The difficult step is to obtain an accurate interatomic potential to use in the $H_{\rm MD}$. While we may do our best to introduce physically realistic potential functions, including many-body terms, calibrating it to band-structure calculations is a powerful procedure for overcoming defects in the form of the potential function. In principle, if the form of the interatomic potential is correct, calibration to small distortions from a perfect crystal is sufficient. In practice, to be able to treat far-from-crystalline configurations, calibration to a band-structure calculation of an amorphous cluster might prove helpful.

The motivation for this work comes from the need to calculate equations of state and thermodynamic properties for metals under extreme conditions where experimental information is not available. We have therefore developed an *ab initio* procedure, requiring no experimental data whatsoever, and applicable at any density, and at temperatures up to several times melting. Our theoretical results for Al achieved good accuracy and this is possible for other metals as well. Our procedure therefore shows promise to provide reliable information on thermodynamic properties of metals under extreme conditions.

APPENDIX: THERMODYNAMIC FUNCTIONS

Here we give the particular functions used to represent the Helmholtz free energy and the corresponding, thermodynamically consistent functions for pressure and entropy. The latter were used to construct the Gibbs energy of the fcc crystal and liquid phases of aluminum and also the internal energy.

Corresponding to Eq. (20) for the Helmholtz energy, its derivatives are given by

$$PV=-\left[\frac{\partial F}{\partial \ln V}\right]_T=(P_0+P_{\rm MD}+P_E)V\ , \tag{A1}$$

$$TS=-\left[\frac{\partial F}{\partial \ln T}\right]_V=(S_{\rm MD}+S_E)T\ . \tag{A2}$$

The Gibbs energy is then obtained from $G=F+PV$ and the internal energy from $U=F+TS$.

The coefficients of the Birch-Murnaghan fit to the band-structure energy contributions to Eq. (20) are [see Eq. (1)]

$$V_b=106.302a_0^3\ ,\quad c_0=-287.7832\ \text{mRy}\ ,$$
$$c_2=761.2029\ \text{GPa}\ ,\quad c_3=1319.036\ \text{GPa}\ , \tag{A3}$$
$$c_4=-13\,661.06\ \text{GPa}\ ,\quad c_5=50\,315.53\ \text{GPa}\ .$$

For aluminum, the contribution of valence electron excitations to Eq. (20) is

$$F_E=-0.025\,353\,8\times10^{-4}V^{2/3}kT^2\ . \tag{A4}$$

The volume-dependent terms in the thermodynamic functions for the crystal, Eqs. (11)–(15), which were obtained by fitting Eqs. (13) and (15) to the MD results, are

$$A^c=4.14\times10^{-10}-8.7\times10^{-12}V+4\times10^{-14}V^2\ , \tag{A5}$$

$$\frac{dA^c}{d\ln V}=-8.7\times10^{-12}V+8\times10^{-14}V^2\ , \tag{A6}$$

$$\gamma_0=0.0803+0.0142V+2\times10^{-5}V^2\ , \tag{A7}$$

$$\ln\theta=7.7217-0.0803\ \ln V-0.0142V-1\times10^{-5}V^2\ . \tag{A8}$$

The pressure and internal energy in the liquid, consistent with Eq. (16), are given by

$$VP^l_{\rm MD}=-\frac{\partial\chi_0}{\partial\ln V}+3kT\gamma_0^l-\frac{\partial A^l}{\partial\ln V}T^3\ , \tag{A9}$$

$$U^l_{\rm MD}=\chi_0+3kT-2A^lT^3\ , \tag{A10}$$

respectively. Fitting these expressions to the MD results provides the volume-dependent terms in Eqs. (16), (17), (A9), and (A10):

$$\chi_0=8.886-0.2914\bar V+2.57\times10^{-3}\bar V^2+5.9\times10^{-5}\bar V^3\ , \tag{A11}$$

$$\frac{1}{V}\frac{\partial\chi_0}{\partial\ln V}=-0.2914+5.14\times10^{-3}\bar V+1.77\times10^{-4}\bar V^2\ , \tag{A12}$$

$$A^l=1.48\times10^{-11}+2.135\times10^{-12}\bar V+4.9\times10^{-14}\bar V^2+2\times10^{-15}\bar V^3\ , \tag{A13}$$

$$\frac{1}{V}\frac{\partial A^l}{\partial\ln V}=2.135\times10^{-12}+9.8\times10^{-14}\bar V+6\times10^{-15}\bar V^2\ , \tag{A14}$$

$$\gamma_0^l=1.5775+5.79\times10^{-3}\bar V+6.5\times10^{-4}\bar V^2\ , \tag{A15}$$

$$\ln\eta_0=41.713\,74-7.831\,46\ln V+0.060\,93\bar V-3.25\times10^{-4}\bar V^2\ . \tag{A16}$$

The units of the quantities in Eqs. (A4)–(A16) are as follows: A^c and A^l are in mRy/K^3; Boltzmann's constant k is in mRy/K; T, θ, and η_0 are in K; V and $\bar V$ are in a_0^3/atom, with $\bar V=V-102.644$; χ_0 is in mRy.

[1]M. Born and R. Oppenheimer, Ann. Phys. **84**, 457 (1927).
[2]D. C. Wallace, *Thermodynamics of Crystals* (Wiley, New York, 1972), Sec. 24.
[3]J. A. Moriarty, D. A. Young, and M. Ross, Phys. Rev. B **30**, 578 (1984).
[4]J. L. Pélissier, Physica A **128**, 363 (1984).
[5]J. Mei and J. W. Davenport, Phys. Rev. B **46**, 21 (1992).
[6]J. M. Wills and B. R. Cooper, Phys. Rev. B **36**, 3809 (1987); Olle Eriksson, J. M. Wills, and A. M. Boring, *ibid.* **46**, 12 981 (1992); J. M. Wills (unpublished).
[7]J. M. Wills, Olle Eriksson, Per Söderlind, and A. M. Boring, Phys. Rev. Lett. **68**, 2802 (1992); Per Söderlind, Olle Eriksson, J. M. Wills, and A. M. Boring, Phys. Rev. B **48**, 5833 (1993).
[8]L. Hedin and B. I. Lundqvist, J. Phys. C **4**, 2064 (1971).
[9]S. Froyen, Phys. Rev. B **39**, 3168 (1989); M. Methfessel and A. T. Paxtaon, *ibid.* **40**, 3616 (1989).
[10]F. Birch, J. Geophys. Res. **83**, 1257 (1978).
[11]D. C. Wallace, Phys. Rev. **187**, 991 (1969).
[12]D. C. Wallace, Phys. Rev. B **1**, 3963 (1970).
[13]D. C. Wallace, Phys. Rev. **182**, 778 (1969); Phys. Rev. B **1**, 942 (1970).
[14]C. J. Pethick, Phys. Rev. B **2**, 1789 (1970).
[15]D. J. W. Geldart and S. H. Vosko, Can. J. Phys. **44**, 2137 (1966); **45**, 2229(E) (1967).
[16]R. E. Swanson, G. K. Straub, B. L. Holian, and D. C. Wallace, Phys. Rev. B **25**, 7807 (1982).
[17]N. W. Ashcroft, Phys. Lett. **23**, 48 (1966).
[18]A. K. McMahan and J. A. Moriarty, Phys. Rev. B **27**, 3235 (1983).
[19]P. K. Lam and M. L. Cohen, Phys. Rev. B **27**, 5986 (1983).
[20]T. R. Koehler, N. S. Gillis, and D. C. Wallace, Phys. Rev. B **1**, 4521 (1970).
[21]D. C. Wallace, Proc. R. Soc. London Ser. A **433**, 631 (1991).
[22]D. C. Wallace, *Thermodynamics of Crystals* (Ref. 2), Sec. 19.
[23]H. Schober and P. H. Dederichs, in *Metals: Phonon States, Electron States and Fermi Surfaces,* edited by K.-H. Hellwege and J. L. Olsen, Landolt-Börnstein, New Series, Group III, Vol. 13, Pt. a (Springer-Verlag, Berlin, 1981).
[24]G. K. Straub and D. C. Wallace, Phys. Rev. B **30**, 3929 (1984).
[25]S. K. Schiferl and D. C. Wallace, Phys. Rev. B **31**, 7662 (1985).
[26]G. K. Straub, S. K. Schiferl, and D. C. Wallace, Phys. Rev. B **28**, 312 (1983).
[27]B. L. Holian, G. K. Straub, R. E. Swanson, and D. C. Wallace, Phys. Rev. B **27**, 2873 (1983).
[28]D. C. Wallace, B. L. Holian, J. D. Johnson, and G. K. Straub, Phys. Rev. A **26**, 2882 (1982).
[29]D. C. Wallace and G. K. Straub, Phys. Rev. A **27**, 2201 (1983).
[30]D. C. Wallace, S. K. Schiferl, and G. K. Straub, Phys. Rev. A **30**, 616 (1984).
[31]D. C. Wallace, Phys. Rev. **176**, 832 (1968).
[32]S. K. Schiferl and D. C. Wallace, J. Chem. Phys. **83**, 5203 (1985).
[33]D. C. Wallace, Phys. Rev. B **46**, 5242 (1992).
[34]C. Sanchez-Castro, J. B. Aidun, G. K. Straub, J. M. Wills, and D. C. Wallace, Phys. Rev. A (to be published).
[35]A. J. Leadbetter, J. Phys. C **1**, 1489 (1968).
[36]J. Rosén and G. Grimvall, Phys. Rev. B **27**, 7199 (1983).
[37]See Ref. 2, Table 12; also Ref. 21, Table 2.